NASA Research Grant/Cooperative Agreement NCC1-02018

Principal Investigator: Dr. Nikita S. Pougatchev

Christopher Newport University

1 University Place

Newport News, VA 23606

Final Report

INTRODUCTION

Carbon monoxide is considered mission critical (TRACE-P NRA) because it is one of the gases involved in controlling the oxidizing power of the atmosphere and, as a tracer gas, is valuable in interpreting mission data sets. Carbon monoxide exhibits interannual differences, suggesting relatively short-term imbalances in sources and sinks [Novelli et al., 1998b]. Sources of CO are dominated by fossil fuel combustion, biomass burning, and the photochemical oxidation of CH_4 and nonmethane hydrocarbons while reaction with OH is believed to be the major sink for atmospheric CO, with additional losses due to soil uptake [Logan et al., 1981 and Bawkin et al., 1994]. Uncertainties in the magnitude and distribution of both sources and sinks remain fairly large however, and additional data are required to refine the global budget. Seasonal changes and a northern hemispheric latitudinal gradient have been described for a variety of Pacific basin sites through long-term monitoring of surface background levels [Novelli et al., 1998b]. Latitudinal variations have also recently been described at upper tropospheric altitudes over a multi-year period by Matsueda et al., 1998.

TRACE-P will provide an aircraft survey of CO over the northern Pacific in the northern spring when CO concentrations are at their seasonal maximum in the northern hemisphere (NH) and at their seasonal minimum in the southern hemisphere (SH). Previous GTE missions, i.e., PEM West-B and PEM Tropics-B, ground-based, and satellite observations (MAPS, April 1994) give us a general picture of the distribution of CO over the northern Pacific during this season. Based on these measurements, background CO levels over remote ocean areas are anticipated to be in the range of 110 - 180 ppbv, while those closer to the Asian continent may rise as high as 600 ppbv [Talbot et al., 1997; Novelli et al., 1998a, b; Connors et al., 1999]. These measurements also reveal high spatial variability (both horizontal and vertical) as well as temporal variations in CO over the area planned for the TRACE-P mission. This variability is a result of multiple CO sources, the meteorological complexity of transport processes, and the photochemical aging of air masses. The influence of biomass burning in the southern Pacific should be relatively small since the mission coincides with the southern tropical wet season when agricultural burning is at its seasonal low [Hao and Ward, 1994; Brocard et al., 1998]. The proposed CO measurements taken during TRACE-P should therefore largely be a function of the impact of various NH sources, primarily Asian and predominantly fossil fuel combustion and biomass burning. These processes are also major sources of many other atmospheric pollutants, consequently making accurate and precise CO measurements is one of the highest TRACE-P priorities [TRACE-P NRA]. The TRACE-P mission emphasizes the dual objectives of assessing the magnitude of the transport of chemically and radiatively important gases such as CO from Asia to the western Pacific, and determining how emissions change and are modified during this transport.

SATELLITE and GROUND-BASED MEASUREMENTS\

FTIR measurements were performed during all the MOPITT's science phases and are in progress now. The FTIR data were used to validate the satellite CO retrievals and some results are presented in Figure 1. Agreement is good and systematic differences between two data sets are statistically insignificant.

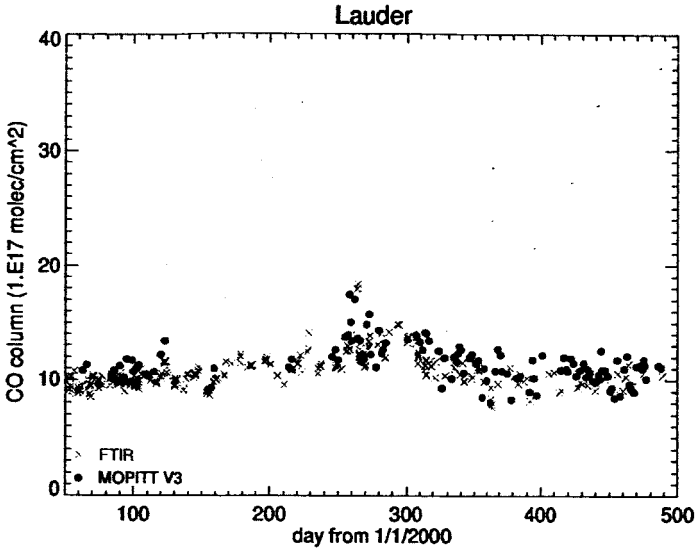

Figure 1a. CO total column measured by the MOPITT (version 3 of Level 2 data processing) and ground-based FTIR technique at Lauder, New Zealand, 45° S, 169.8° E.

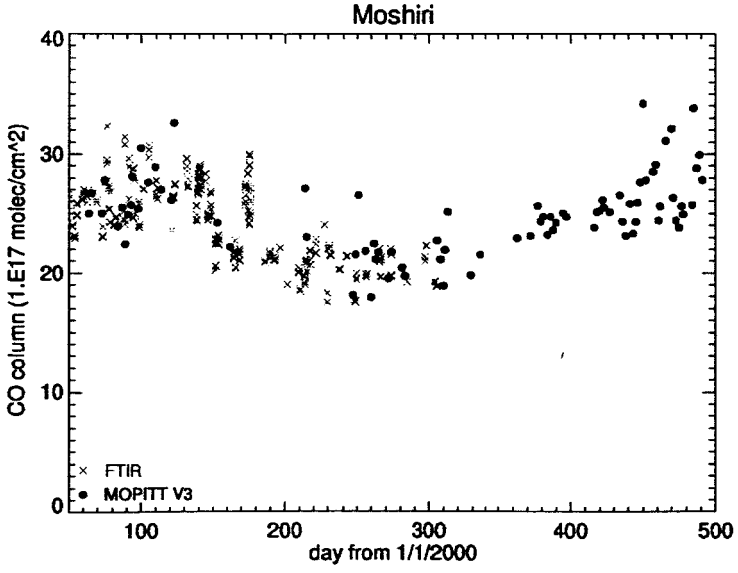

Figure 1b. CO total column measured by the MOPITT (version 3 of Level 2 data processing) and ground-based FTIR technique at Moshiri, Japan, 44.4° N, 142.3° E.

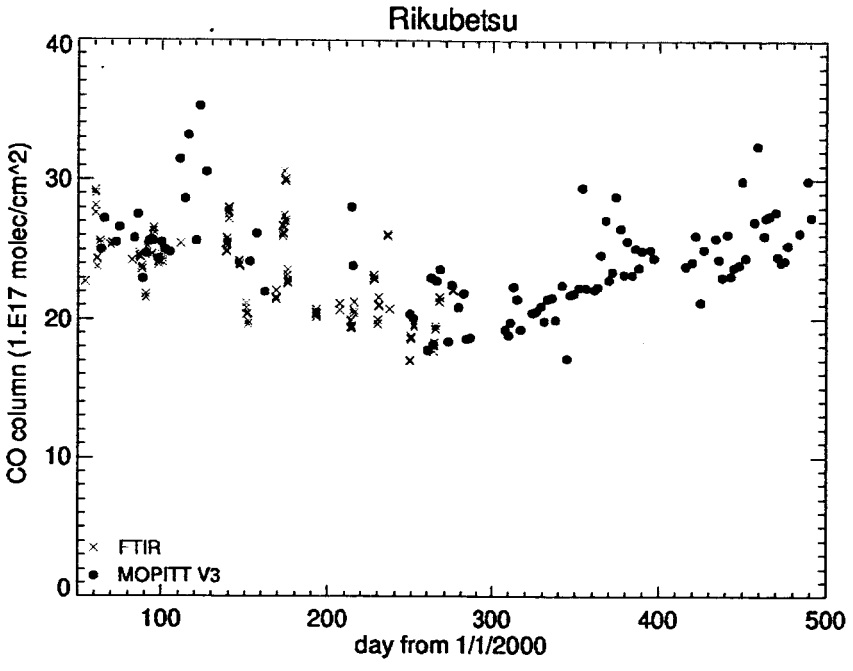

Figure 1c. CO total column measured by the MOPITT (version 3 of Level 2 data processing) and ground-based FTIR technique at Rikubetsu, 43.5° N, 143.8° E.

The displayed results characterize seasonal and irregular variations of the CO total column in the northern and southern hemispheres. Work on the validation of the profile retrievals is in progress now.

ARCRAFT MEASUREMENTS

The purpose of this work is to analyze ozone and CO vertical profiles retrieved from NAST-I spectra. Retrievals were validated against in situ CO and ozone measurements made by two sensors flown aboard BW57 aircraft. For analysis we used two approaches, namely, statistical and case study.

In statistical approach we used eigenvector analysis to determine how well retrievals can reproduce vertical structure of in situ profiles and we also estimated

vertical resolution of the retrievals. We used atmospheric structure function approach to determine how much of horizontal variability can be captured by retrievals.

In the case study we analyzed retrievals from spectra taken during one flight on July 19, 2002. The particular flight was selected for analyses because of some peculiar features in CO, ozone and H_2O distribution were observed in retrievals. We analyzed relations between those parameters and compared them to in situ data. We also used backward trajectories analysis to explain the observed phenomena.

Both approaches show that ozone retrievals are in a good agreement with the data available for comparison and validation. Vertical resolution of the ozone profile was estimated to be between 4 km and 5 km. We also demonstrated that ozone retrievals provide additional information about atmospheric motion.

Analysis of the CO retrievals was limited to qualitative comparison due to significantly smaller (comparatively to the ozone) amount of in situ data available for reliable validation. More work is needed in this area involving in situ measurement from different campaigns, e. g., TRACE-P.

DATA DESCRIPTION

In situ data. Most part of the flights was at altitudes higher that 8 km, which means that profiles could be taken during the take off ascent and landing descent. Total 26 in situ profiles are available for the analysis. Ozone measurements were made at all altitudes, CO sensor could operate only above 7 km. Campaign average ozone and CO profiles are presented on Figures 2, 3. Each data point on the profiles represent volume mixing ratio (VMR) averaged within 500m thick layers. Error bars indicate standard deviation.

Retrievals. Ozone, CO, and H_2O profiles were retrieved from NAST-I spectra at cruise altitude of the PROTEOUS airplane 15 – 18 km. Examples of the retrieved data are presented in Figure 4, 5, and 6. The blank area on the color plates indicates a segment of the flight where cloud contamination was detected.

Detailed discussion of the data will be presented in the following sections.

STATISTICAL APPROACH

Eigenvector analysis. Eigenvector analysis allows us to estimate what spatial vertical frequencies (wavelength) are present in retrieved and in situ profiles, and what is their intensity. We calculated covariance matrix for 26 available in situ ozone profiles (2 profiles per flight) and covariance matrix for all retrieved profiles taken along cloud free segments of three NAST-I flights performed on July 9-th, 19-th, and 26-th. Then corresponding eigenvectors and eigenvalues were calculated. The results are presented on Figures 7, 8. It can be seen that first four eigenvectors as well as 3 eigenvalues are in a reasonable agreement what is an indicator of what spatial frequencies in the ozone true vertical distribution can be captured by the NAST-I retrievals.

Vertical resolution. In the process of the current work we develop a technique for estimation of a vertical resolution of the retrievals. The technique is based on a comparative analysis of off-diagonal elements in the in situ and retrieval covariance matrices. Finite resolution of the retrievals causes stronger correlation between points in a retrieved profile what results in relatively larger off-diagonal elements in retrieval covariance matrix. Using this technique we estimated that the *NAST-I ozone retrieval vertical resolution is approximately 4 km.*

Ozone structure function. Atmospheric structure function is an important and powerful tool for statistical describing and studying atmospheric advection, or, in other words horizontal motion. For the true two dimensional turbulence according to Obukhov-Corsin relation

$$<dQxdQ>=C*R^{2/3}$$

Where <dQ*dQ> is a second order structure function for a passive scalar Q (in our case it is ozone vmr), C is a constant which magnitude depends on some specific conditions, and R is a separation between two points. If we are dealing with atmospheric layers of finite thickness we have a similar relation but $<dQxdQ>=C*R^x$ where $x<2/3$. In practice we always are dealing with the layers of finite thickness, in particular, if those are remote sensing data. Therefore, if we would like to compare NAST-I and in situ structure functions, the in situ structure function must be calculated for a layer which thickness is comparable with the NAST-I vertical resolution. We calculated structure functions for 14 – 16 km layer of in situ data and the NAST-I retrievals at 125 mb level. Both sets of data represent the ozone in the lower stratosphere. Results are presented in Figure 9. In the range between 2 – 100 km, and 100 –200 km slopes of both curves are very close (black and blue lines are parallel respectively), and behavior of the curves is similar. Structure function for the retrieval data is noisier, what can be explained by smaller number of measured data points. *Thus, we can make a conclusion that the NAST-I is capable to capture reliably small and mesoscale horizontal atmospheric motion in layers ~2km thick or larger.*

CASE STUDY.

The purpose of the case study is to look at some particular details observed by NAST-I during a selected flight and interpret them using independent meteorological information, in situ measurement, and correlation between measured species.

For the case study we selected one NAST-I flight performed on July 19 2002. Analyzed segment of the flight was mainly in South-North-South direction, over the Atlantic Ocean off coast of Florida. The particular flight was selected for analyses because of some peculiar features in CO, ozone and H_2O distribution were observed in retrievals. In particular, *Ozone (Figure 4)* (i) stable layer with enhanced ozone between 600 mb and 400 mb, (ii) apparent descent of high troposphere ozone starting at ~ 29° N, (see Figure. 4); *Water vapor* (i) relatively dry area between 600 mb and 400 mb at the southern (24°N –25.5°N) and northern (30°N – 31°N) segments of the flight (see Figure 11); *CO* It can be seen from color pallet in Figure 5 that between 24°N – 26° N lower and mid troposphere is less polluted then at altitudes higher than 29°N, the plot in Figure 12 illustrates this observation in a quantitative manner.

Comparison to in situ There are two in situ ozone profiles on July 19 2002. In Figure 13 they are shown along with the retrieved profile averaged along the flight. As one can judge, agreement is good and the "layer" with enhanced ozone between 400 mb and 600 mb is presented in both in situ and retrieved profiles.

Backward trajectory analysis We calculated 5 days backward trajectories for two locations, i. e., 25.8° N, 80.3°W (south end of the flight) and 30.5°N, 81.7°W (north end of the flight). The trajectories are presented Figures 14, 15. The air in the area of southern part of the flight came from the Atlantic Ocean where there are no any sources of

pollution. The air, which arrived to the area of northern part of the flight, spent several days over heavily industrialized and polluted part of the Southern part of the US. That supports the observed increase of CO concentration while going north.

Correlation between components. As it was established in previous studies, ozone in polluted air is produced at significant rates. CO is one of the major indicators of pollution, therefore, one might expect significant correlation between CO and ozone in an airmass, which came from obviously polluted regions. In Figure 16 we plotted retrieved CO vs retrieved ozone. As one can judge, strong correlation is observed with correlation coefficient ~0.75. This is an indicator that at least some fraction of elevated ozone in the northern segment of the flight was cased by photochemical production under polluted conditions.

Scatter plot in Figure 17 demonstrates correlation between retrieved ozone and H_2O mixing ratios at 500 mb level. Strong correlation is observed in the area of the plot where ozone vmr is higher than ~0.06 ppmv and H_2O mr is less than ~1 g/kg. These conditions were observed at the segment of the flight north off ~ 26°N. Looking at the color plate in Figure 4 one can notice that this is the area where apparent ozone subsidence was observed. In other words, ozone-reach-water-poor air from higher altitudes descended what contributed to ozone enhancement in the northern segment of the flight.

PRELIMINARY CONCLUSIONS

1. Eigenvector analysis of the ozone retrievals indicates that NAST-I is capable to capture major features in the ozone vertical distribution in the troposphere and lover stratosphere with vertical resolution of 4 km.
2. Structure function analysis indicates that the NAST-I is capable to capture reliably advective atmospheric motion in the range from the small scale to mesoscale.
3. Statistical analyses of the ozone retrievals and comparison to in situ data show that the NAST-I can be a *powerful tool for validation of satellite tropospheric ozone retrievals* as well as independent research instrument.
4. Case study demonstrates that ozone, CO, and H_2O retrievals are internally consistent and are in a reasonable agreement with independent information. Simultaneous measurements of the mentioned above components significantly enhance NAST-I capability to measure atmospheric motion of various scales.
5. The scope of performed study was limited by the data set from one field campaign only, and for reliable validation further work, involving more extensive data sets, e. g., TRACE-P, is required.

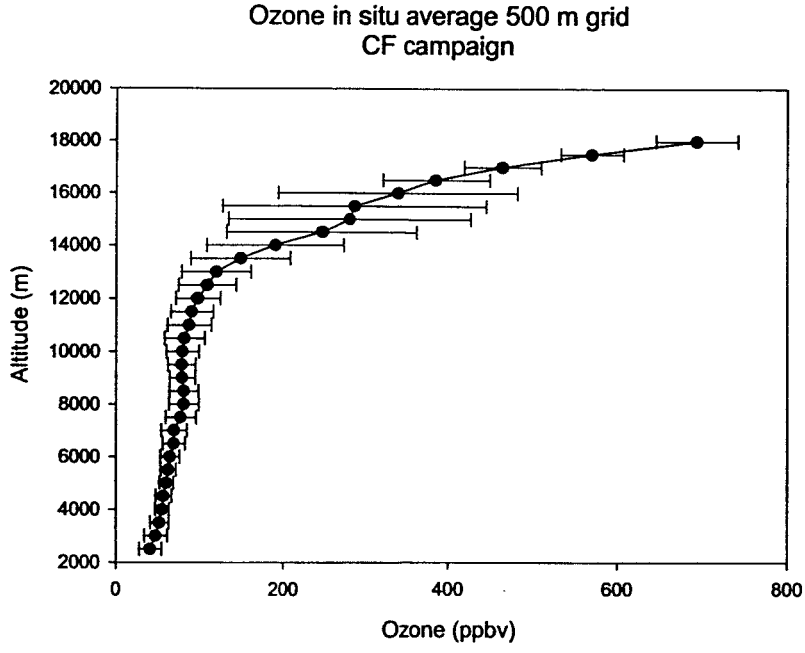
Ozone in situ average 500 m grid
CF campaign
Altitude (m)
20000
18000
16000
14000
12000
10000
8000
6000
4000
2000
0
200
400
600
800
Ozone (ppbv)

Figure 2

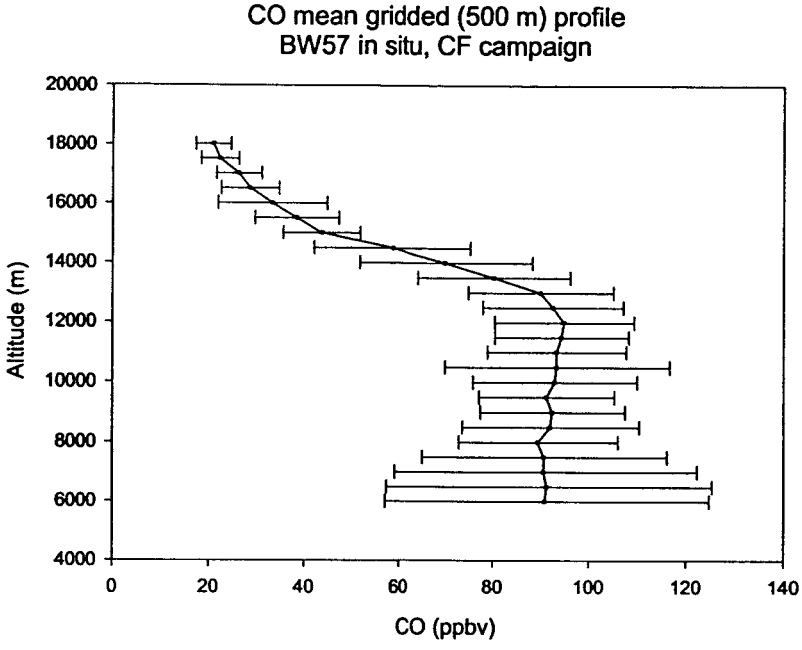
CO mean gridded (500 m) profile
BW57 in situ, CF campaign
Altitude (m)
20000
18000
16000
14000
12000
10000
8000
6000
4000
0
20
40
60
80
100
120
140
CO (ppbv)

Figure 3

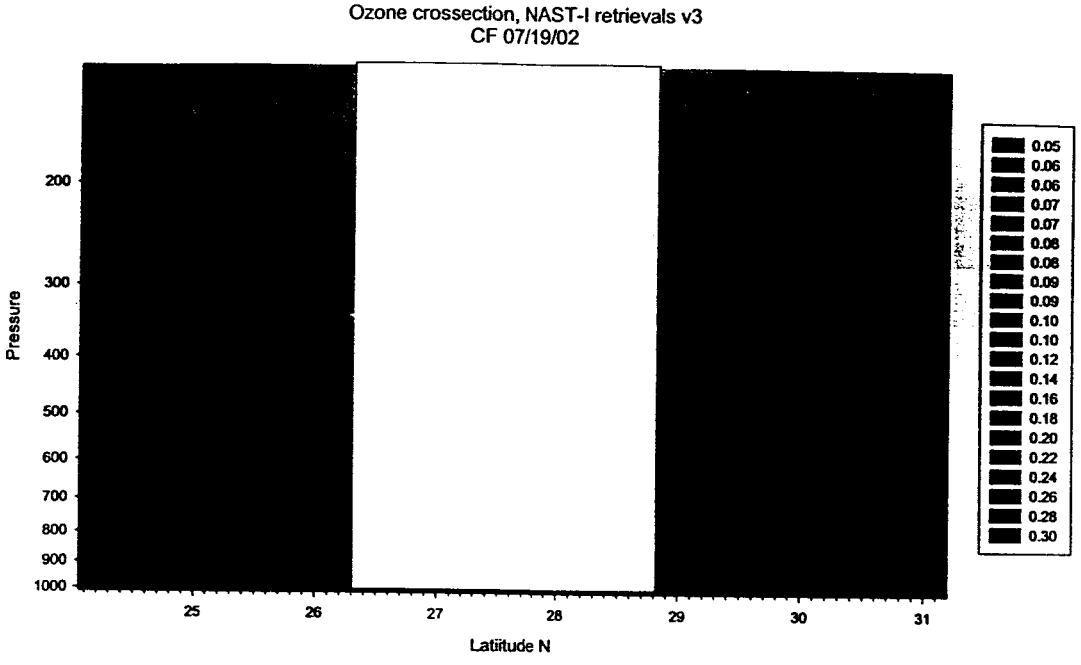
Ozone crossection, NAST-I retrievals v3
CF 07/19/02
Pressure
200
300
400
500
600
700
800
900
1000
25
26
27
28
29
30
31
Latiitude N
0.05
0.06
0.06
0.07
0.07
0.08
0.08
0.09
0.09
0.10
0.10
0.12
0.14
0.16
0.18
0.20
0.22
0.24
0.26
0.28
0.30

Figure 4

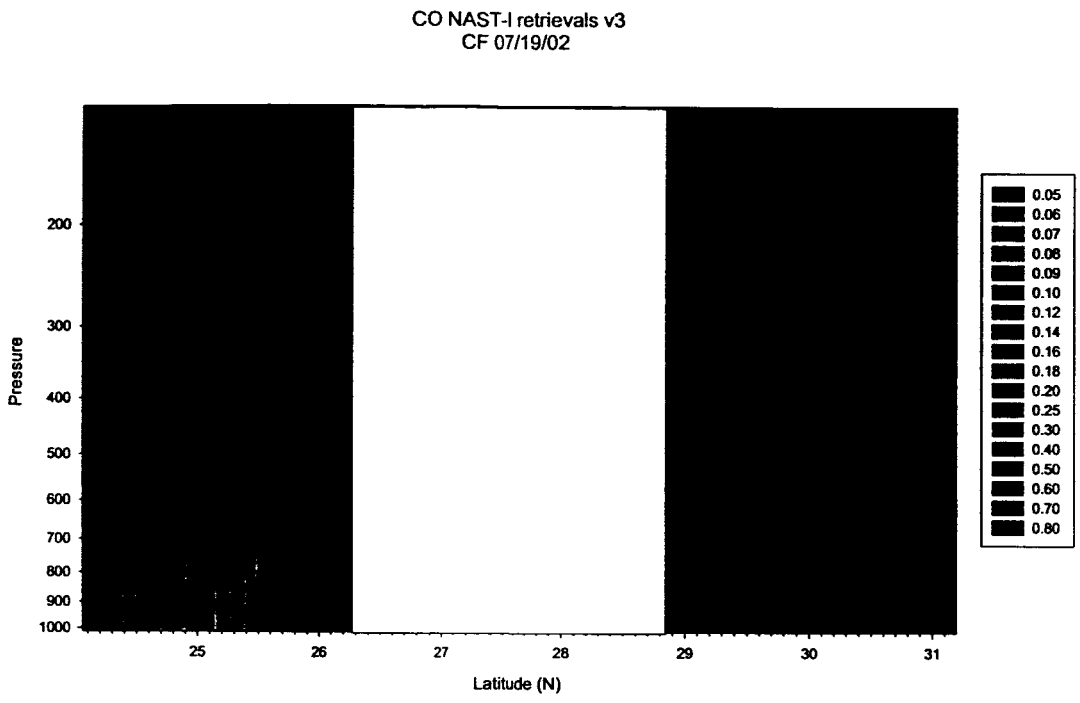
CO NAST-I retrievals v3
CF 07/19/02
Pressure
200
300
400
500
600
700
800
900
1000
25
26
27
28
29
30
31
Latitude (N)
0.05
0.06
0.07
0.08
0.09
0.10
0.12
0.14
0.16
0.18
0.20
0.25
0.30
0.40
0.50
0.60
0.70
0.80

Figure 5

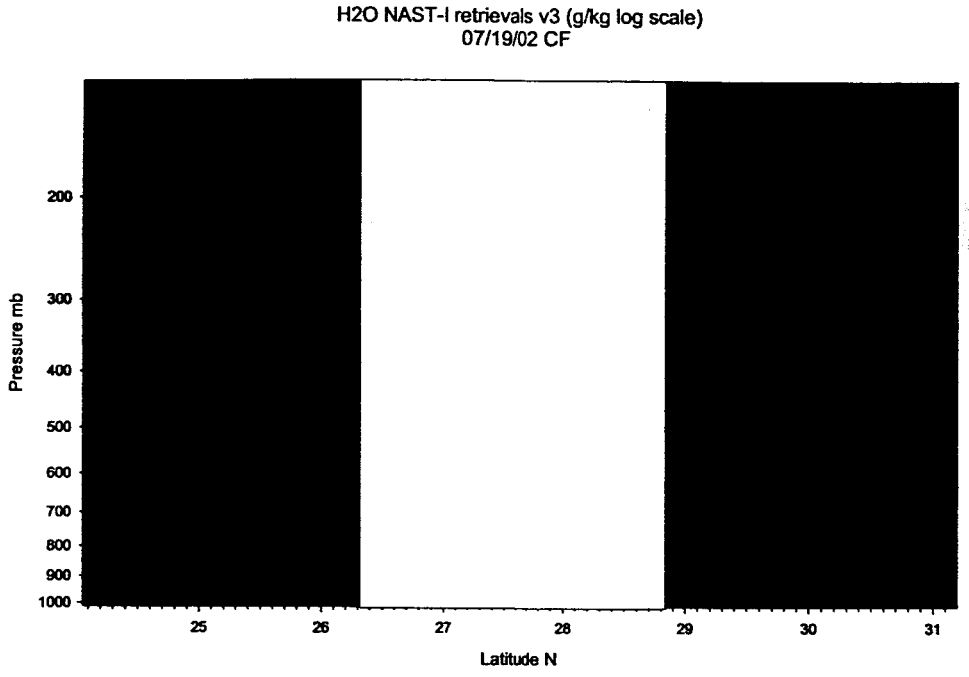
H2O NAST-I retrievals v3 (g/kg log scale)
07/19/02 CF
Pressure mb
200
300
400
500
600
700
800
900
1000
25
26
27
28
29
30
31
Latitude N

Figure 6

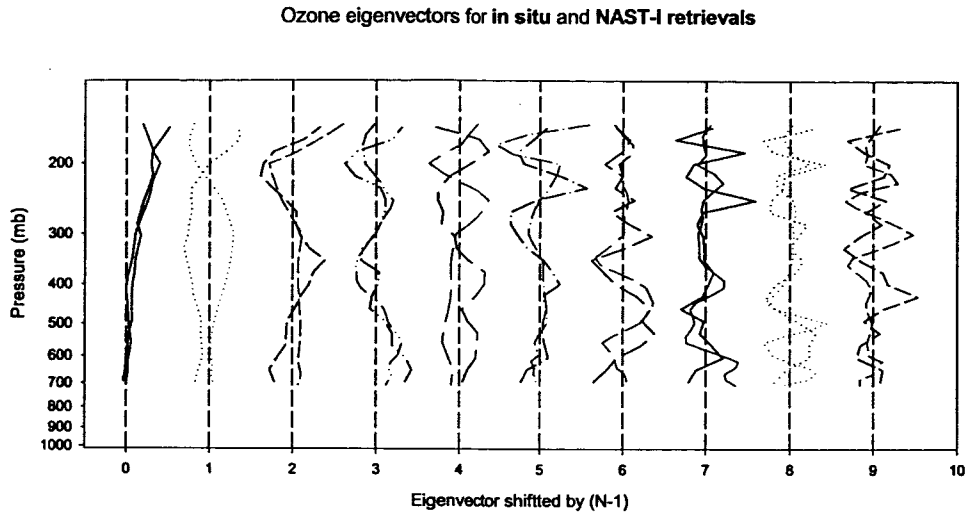
Ozone eigenvectors for in situ and NAST-I retrievals
Pressure (mb)
200
300
400
500
600
700
800
900
1000
0
1
2
3
4
5
6
7
8
9
10
Eigenvector shiftted by (N-1)

Figure 7

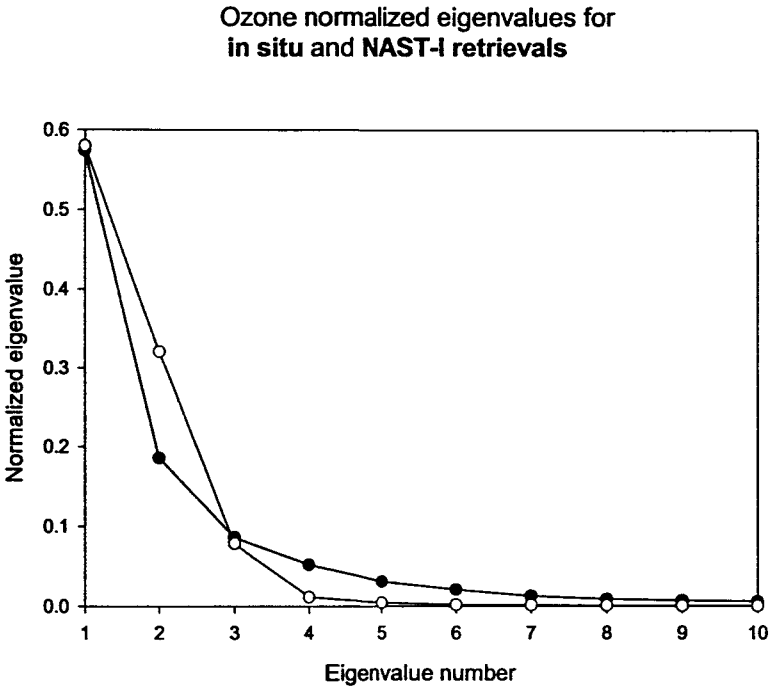
Ozone normalized eigenvalues for
in situ and NAST-I retrievals
Normalized eigenvalue
0.6
0.5
0.4
0.3
0.2
0.1
0.0
1
2
3
4
5
6
7
8
9
10
Eigenvalue number

Figure 8

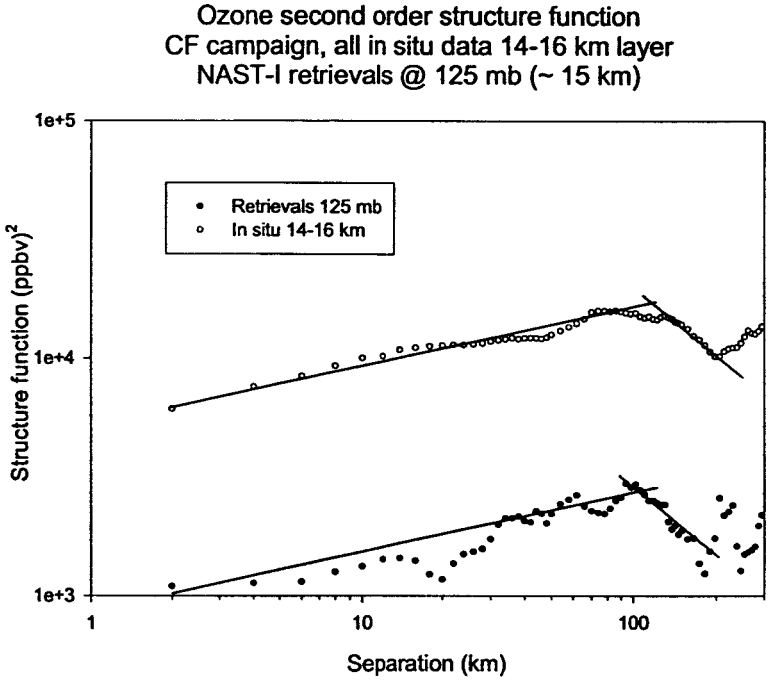
Ozone second order structure function
CF campaign, all in situ data 14-16 km layer
NAST-I retrievals @ 125 mb (~ 15 km)
1e+5
1e+4
1e+3
Structure function (ppbv)²
Retrievals 125 mb
In situ 14-16 km
1
10
100
Separation (km)

Figure 9

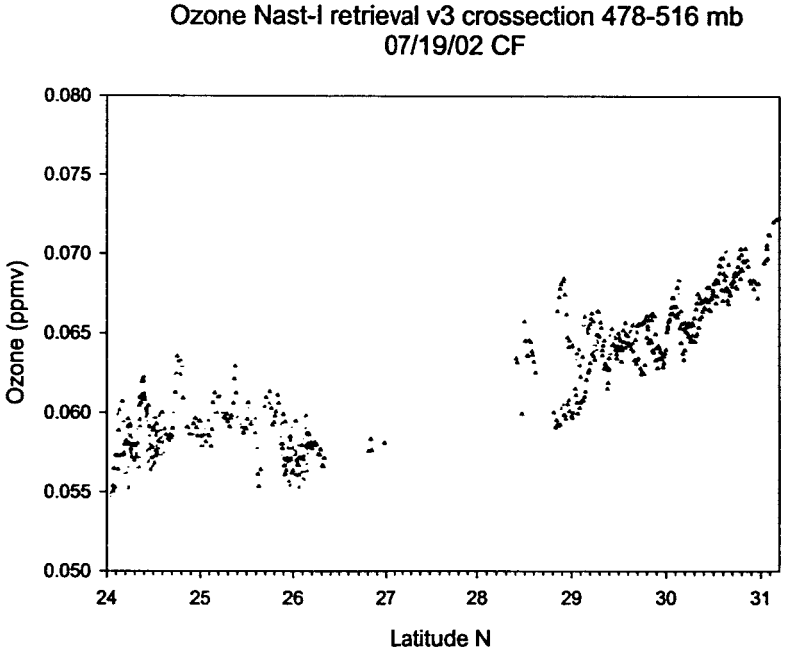
Ozone Nast-I retrieval v3 crossection 478-516 mb
07/19/02 CF
Ozone (ppmv)
0.080
0.075
0.070
0.065
0.060
0.055
0.050
24
25
26
27
28
29
30
31
Latitude N

Figure 10

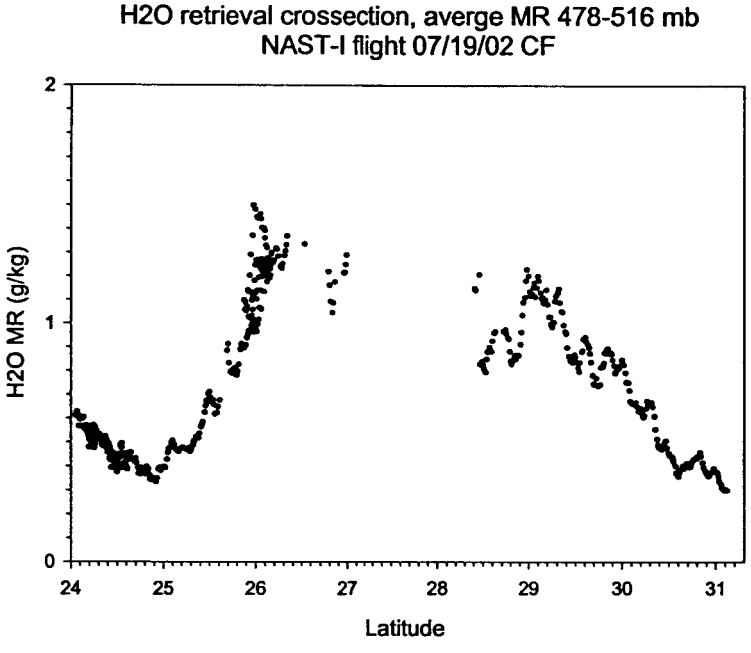
H2O retrieval crossection, averge MR 478-516 mb
NAST-I flight 07/19/02 CF
H2O MR (g/kg)
2
1
0
24
25
26
27
28
29
30
31
Latitude

Figure 11

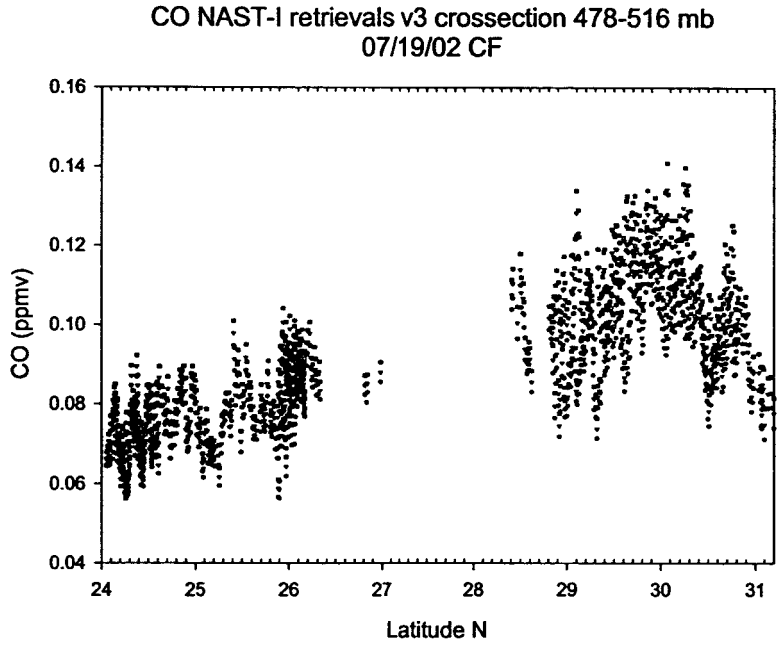
CO NAST-I retrievals v3 crossection 478-516 mb
07/19/02 CF
CO (ppmv)
0.16
0.14
0.12
0.10
0.08
0.06
0.04
24
25
26
27
28
29
30
31
Latitude N

Figure 12

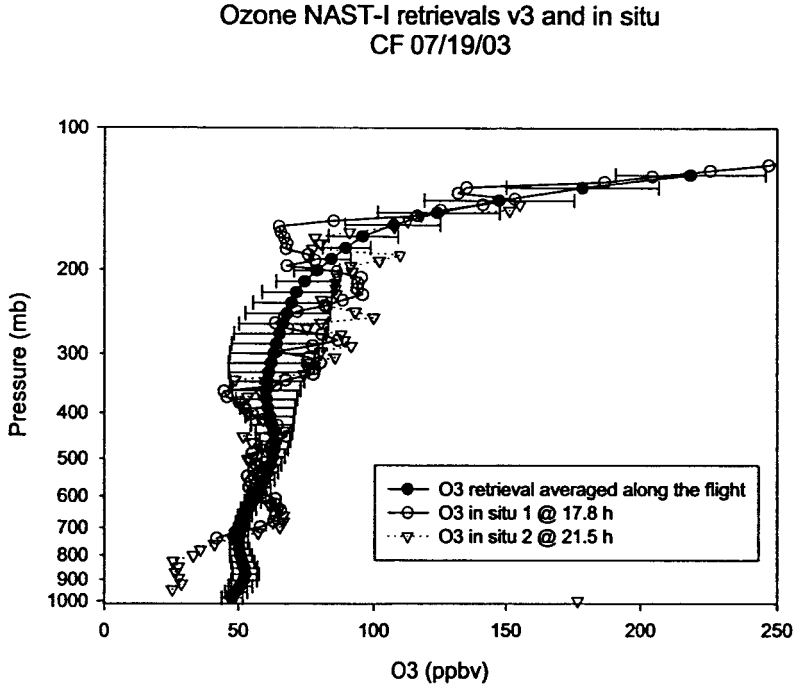
Ozone NAST-I retrievals v3 and in situ
CF 07/19/03
Pressure (mb)
100
200
300
400
500
600
700
800
900
1000
0
50
100
150
200
250
O3 (ppbv)
O3 retrieval averaged along the flight
O3 in situ 1 @ 17.8 h
O3 in situ 2 @ 21.5 h

Figure 13

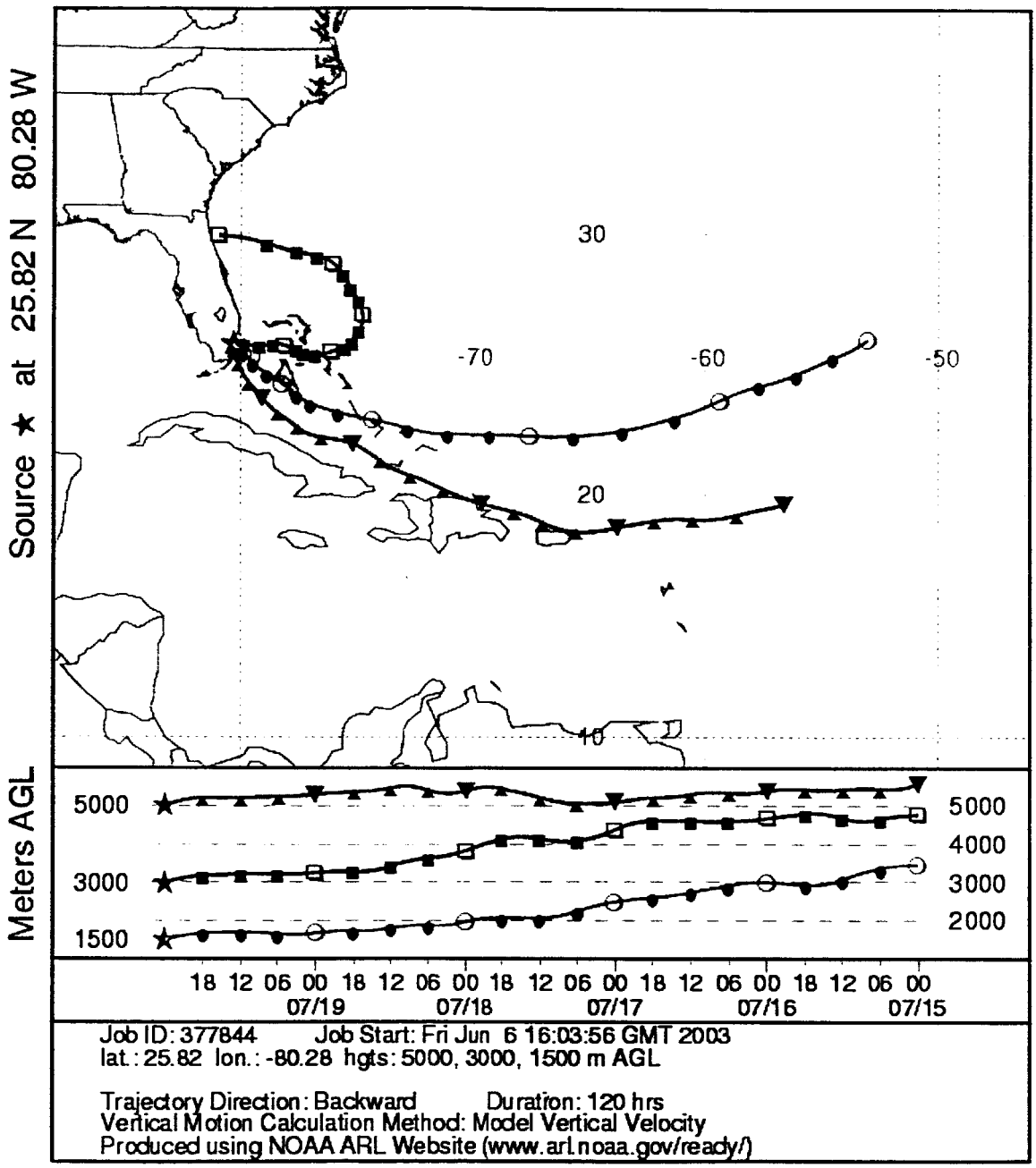
NATIONAL OCEANIC ATMOSPHERIC ADMINISTRATION
Backward trajectories ending at 00 UTC 20 Jul 02
CDC1 Meteorological Data
Source ★ at 25.82 N 80.28 W
30
-70
-60
-50
20
10
Meters AGL
5000
3000
1500
5000
4000
3000
2000
18 12 06 00 18 12 06 00 18 12 06 00 18 12 06 00 18 12 06 00
07/19
07/18
07/17
07/16
07/15
Job ID: 377844 Job Start: Fri Jun 6 16:03:56 GMT 2003
lat.: 25.82 lon.: -80.28 hgts: 5000, 3000, 1500 m AGL
Trajectory Direction: Backward Duration: 120 hrs
Vertical Motion Calculation Method: Model Vertical Velocity
Produced using NOAA ARL Website (www.arl.noaa.gov/ready/)

Figure 14

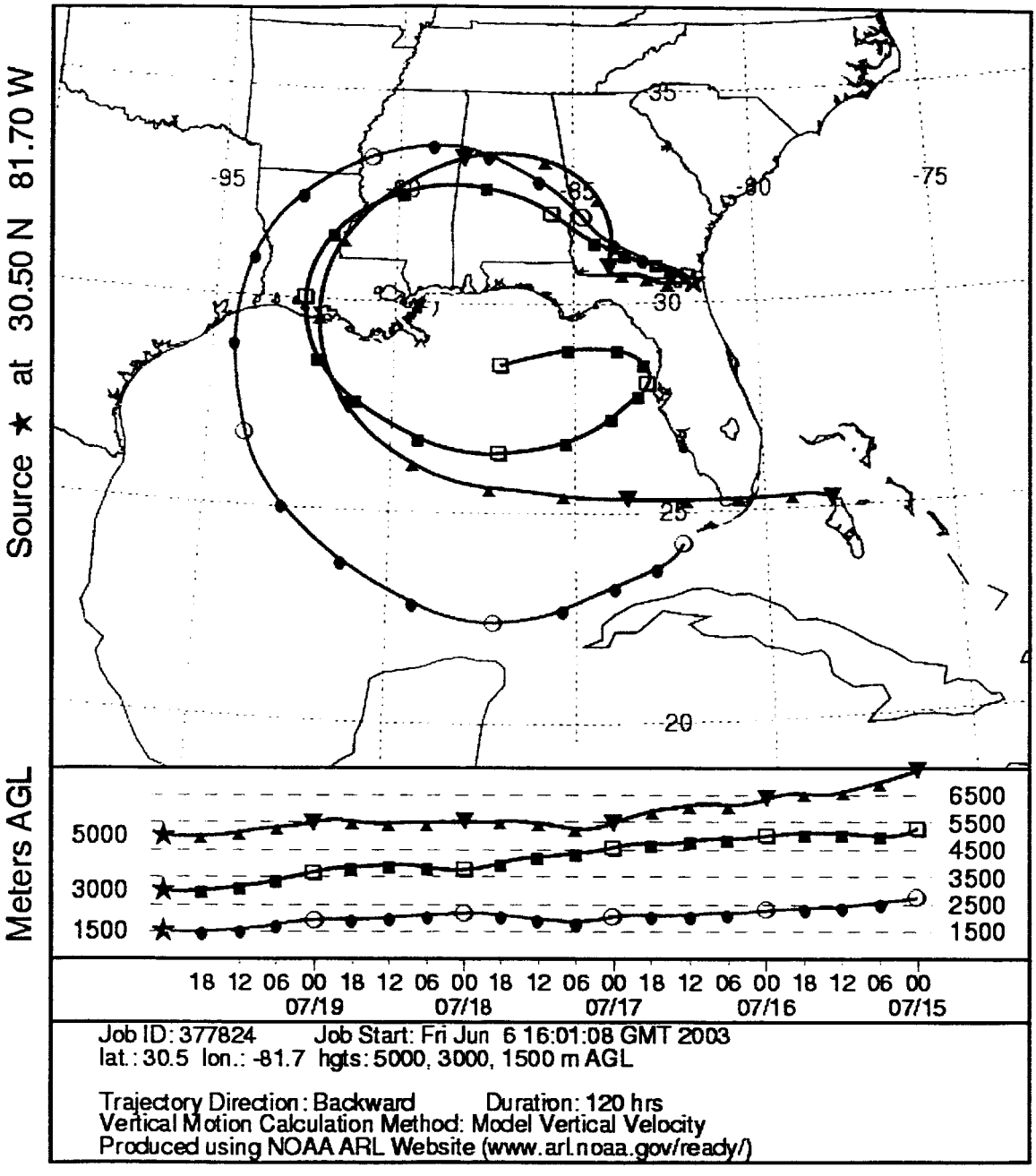
NATIONAL OCEANIC ATMOSPHERIC ADMINISTRATION
Backward trajectories ending at 00 UTC 20 Jul 02
CDC1 Meteorological Data
Source ★ at 30.50 N 81.70 W
Meters AGL
5000
3000
1500
6500
5500
4500
3500
2500
1500
18 12 06 00 18 12 06 00 18 12 06 00 18 12 06 00 18 12 06 00
07/19 07/18 07/17 07/16 07/15
Job ID: 377824 Job Start: Fri Jun 6 16:01:08 GMT 2003
lat.: 30.5 lon.: -81.7 hgts: 5000, 3000, 1500 m AGL
Trajectory Direction: Backward Duration: 120 hrs
Vertical Motion Calculation Method: Model Vertical Velocity
Produced using NOAA ARL Website (www.arl.noaa.gov/ready/)

Figure 15

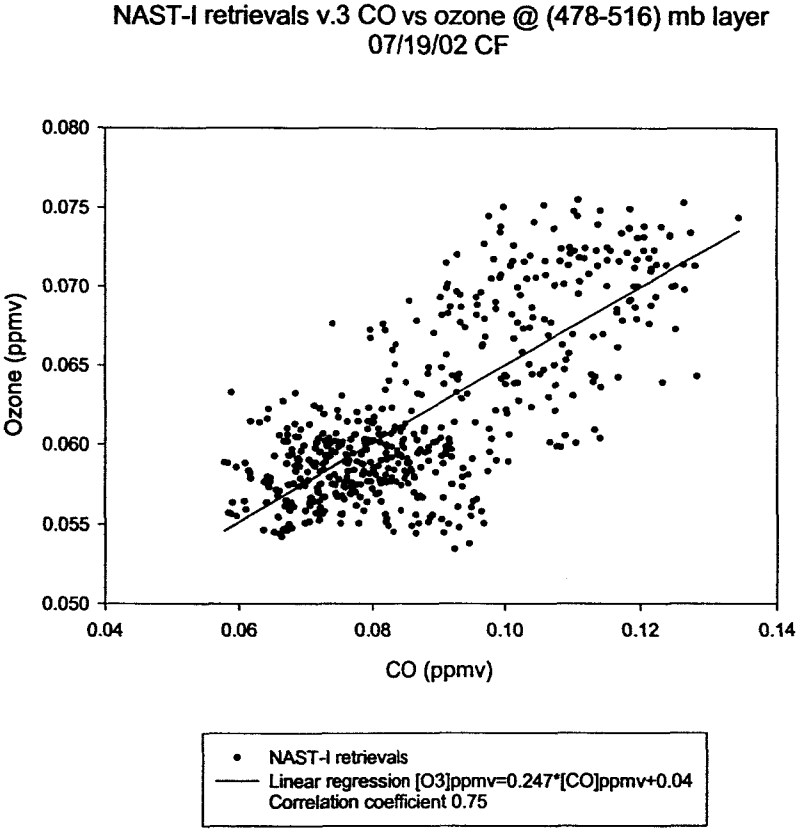
NAST-I retrievals v.3 CO vs ozone @ (478-516) mb layer
07/19/02 CF
0.080
0.075
0.070
0.065
0.060
0.055
0.050
Ozone (ppmv)
0.04
0.06
0.08
0.10
0.12
0.14
CO (ppmv)
NAST-I retrievals
Linear regression [O3]ppmv=0.247*[CO]ppmv+0.04
Correlation coefficient 0.75

Figure 16

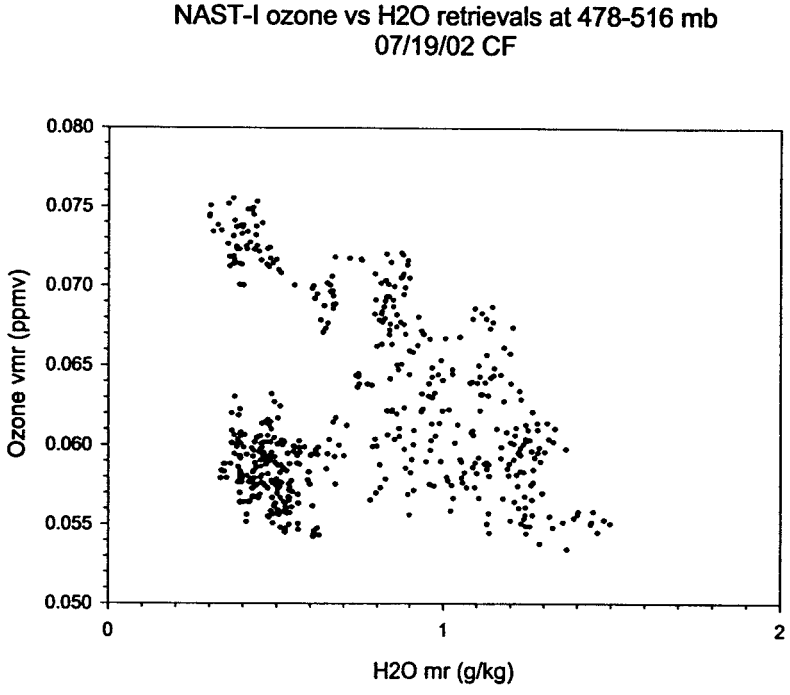
NAST-I ozone vs H2O retrievals at 478-516 mb
07/19/02 CF
0.080
0.075
0.070
0.065
0.060
0.055
0.050
Ozone vmr (ppmv)
0
1
2
H2O mr (g/kg)

Figure 17

References

Bakwin, P.S., P.P. Tans, and P.C. Novelli, Carbon monoxide budget in the northern hemisphere, Geophys. Res., Lett., 21, 433-436, 1994.

Brocard, D., J.P. Lacaux, and H. Eva, 1998, Domestic biomass combustion and associated atmospheric emissions in West Africa, Global Biogeochem. Cycles, 12, 127-139.

Connors, V. S., B. B. Gormsen, S. Nolf, and H. G. Reichle Jr., Spaceborne observations of the global distribution of carbon monoxide in the middle troposphere during April and October 1994, J. Geophys. Res., 104, 21,455 – 21,470, 1999.

Hao, W.M. and M.-H. Liu, Spatial and temporal distribution of tropical biomass burning, Global Biogeochem. Cycles, 8, 495-503.

Logan, J.A., M.J. Prather, S.C. Wofsy, and M.B. McElroy, Tropospheric chemistry: A global perspective, J. Geophys. Res., 86, 7210-7254, 1981.

Matsueda, H., H.Y. Inoue, Y.Sawa, and Y. Tsutsumi, 1998, Carbon monoxide in the upper troposphere over the western Pacific between 1993 and 1996, j. Geophys. Res., 103, 19,093-19,110.

Novelli, P. C., et al., An internally consistent set of globally distributed atmospheric carbon monoxide mixing ratios developed using results from an intercomparison of measurements, J. Geophys. Res., 103, 19,285 – 19,293, 1998.

Novelli, P. C., K. A. Masarie, and P. M. Lang, Distribution and recent changes of carbon monoxide in the lower troposphere, J. Geophys. Res., 103, 19,015 – 19,033, 1998b.

Talbot, R. W., J. E. Dibb, B. L. Lfer, J. D. Bradshaw, S. T. Sandholm, D. R. Blake, N. J. Blake, G. W. Sachse, J. E. Collins Jr., B. G. Heikes, J. T. Merrill, G. L. Gregory, B. E. Anderson, H. B. Singh, D. C. Thornto, A. R. Bandy, and R. F. Pueshel, Chemical characterization of continental outflow from Asia to the troposphere over the western Pacific Ocean during February – March 1994, Results from PEM-West B, J. Geophys. Res., 102,28,255 – 28,274, 1997.